Available online at www.sciencedirect.com
SCIENCE DIRECT®
Journal of Food Engineering 72 (2006) 293–301
JOURNAL OF FOOD ENGINEERING
www.elsevier.com/locate/jfoodeng

Measurements of heat transfer coefficients within convection ovens

James K. Carson *, Jim Willix, Mike F. North

AgResearch MIRINZ Centre, Private Bag 3123, Hamilton, New Zealand

Received 25 June 2004; accepted 21 December 2004
Available online 17 February 2005

Abstract

Measurements of apparent heat transfer coefficients within a typical domestic fan oven and a commercial batch oven were performed using four different methods: back-calculation from transient temperature data; using heat flux sensors; from the mass-loss rate; a psychrometric method. The majority of the measured data ranged between 15 and 40 $W\,m^{-2}\,K^{-1}$, and were approximately twice as high as predicted by a Nusselt number correlation for laminar flow over flat-plates, which was partially attributable to radiation. Of all the methods, the heat flux sensor was the simplest to use and was the only method which revealed the time-variation in the heat transfer coefficient. However, although it was the least practical to implement, the mass-loss-rate method incorporated the effect of evaporation, and since the data measured by this method were more reliable than the data from the psychrometric method, they would be most useful for modelling cooking processes.

Keywords: Heat transfer coefficient measurement; Convection oven; Cooking

1. Introduction

Consumer trends indicate that the consumption of cooked meat products will increase significantly in popularity within the next 20 years, as part of the trend toward "home meal replacement" (Neff, 1997). Some predictions suggest that as much as 70% of internationally traded meat will be sold in cooked or partially cooked form (Anon., 2001). Typically the objective of a cooking process is to produce meat with desirable sensory qualities (colour, texture, flavour and aroma), while also minimising weight loss and ensuring the destruction of microbial pathogens (Fellows, 2000). With this in mind, a greater understanding of cooking processes is required in order to help food processors identify and implement optimal processing conditions.

Mathematical models of certain meat-cooking processes may be found in the literature, including models for immersion cooking (Burfoot & Self, 1988), contact frying (Dagerskog, 1979; Houšová & Topinka, 1985; Ikediala, Correia, Fenton, & Ben-Abdallah, 1996; Pan, Singh, & Rumsey, 2000), convection oven roasting (Chang, Carpenter, & Toledo, 1998; Chen, Marks, & Murphy, 1999; Obuz, Powell, & Dikeman, 2002; Singh, Akins, & Erickson, 1984), and microwave oven roasting (Verboven, Datta, Anh, Scheerlink, & Nicolaï, 2003). The heat transfer coefficient (h) between the surface of the product and its surroundings is an essential parameter of most heat transfer models. For immersion cooking the heat transfer coefficients are relatively easy to predict or measure (Burfoot & Self, 1988). Experimental and theoretical studies of heat transfer coefficients encountered in contact-frying processes have also been performed (Pan & Singh, 2002; Whichchukit, Zorilla,

* Corresponding author. Tel.: +64 7 838 5372; fax: +64 7 838 5625.
E-mail address: james.carson@agresearch.co.nz (J.K. Carson).
URL: http://www.agresearch.co.nz/fst (J.K. Carson).

0260-8774/$ - see front matter © 2005 Elsevier Ltd. All rights reserved.
doi:10.1016/j.jfoodeng.2004.12.010

Nomenclature

A	surface area (m^2)
B	intercept of transient temperature plot (Eq. (8))
c	specific heat capacity ($J\ kg^{-1}\ K^{-1}$)
C	heat flux sensor calibration factor ($(W\ m^{-2})/\mu V$)
D	diffusion coefficient of water in air ($m^2\ s^{-1}$)
E	heat flux sensor output (μV)
F	radiation view factor
h	heat transfer coefficient ($W\ m^{-2}\ K^{-1}$)
k	thermal conductivity ($W\ m^{-1}\ K^{-1}$)
K	constant defined by Eq. (7) ($Pa\ K^{-1}$)
L	enthalpy of vaporisation of water ($J\ kg^{-1}$)
M	molar mass ($kg\ kmol^{-1}$)
p	saturated vapor pressure (Pa)
P	total pressure (Pa)
q	heat flux ($W\ m^{-2}$)
s	slope of temperature–time graph (s^{-1})
t	time (s)
T	temperature (K or °C)
v	air velocity ($m\ s^{-1}$)
V	volume of sample (m^3)
X	characteristic dimension (m)
Y	fractional unaccomplished temperature change
α	thermal diffusivity ($m^2\ s^{-1}$)
β	root of Eq. (7)
ε	emissivity
θ	heat flux sensor temperature correction factor
κ	mass transfer coefficient ($kg\ m^{-2}\ Pa^{-1}\ s^{-1}$)
μ	viscosity (Pa s)
ρ	density ($kg\ m^{-3}$)
σ	Stefan–Boltzmann constant 5.669×10^{-8} ($W\ m^{-2}\ K^{-4}$)
Φ	mass loss per unit surface area ($kg\ m^{-2}\ s^{-1}$)
Bi	Biot number $[hX/k_{plaster}]$
Fo	Fourier number $[\alpha t/X^2]$
Nu	Nusselt number $[hX/k_{air}]$
Pr	Prandtl number $[c\mu/k]$
Re	Reynolds number $[\rho_{air} vX/\mu]$
Sc	Schmidt number $[\mu/(\rho D)]$

Subscripts

∞	property of bulk air within oven
a	apparent value
c	convection
dew	dew-point
i	initial state
r	radiation
s	sample surface

& Singh, 2001). However there is a paucity of experimental data available for heat transfer coefficients encountered in meat roasting processes.

The aim of the work reported in this paper was to measure apparent heat transfer coefficients within convection ovens by a number of different methods, and to assess the efficacy of each method.

2. Heat transfer coefficient measurement methods

The equation commonly referred to as Newton's Law of Cooling (Eq. (1)) is not so much a law as it is a definition of the heat transfer coefficient (Jakob, 1947).

$$q = h(T_s - T_\infty) \tag{1}$$

It is interesting to read Newton's original statement of this 'law' in this paper *Scala graduum Caloris* (Newton, 1701):

"...there was heated a pretty thick piece of iron red-hot...which was taken out of the fire..., and laid in a cold place, where the wind blew continually upon it... the time of its cooling was marked... the excess of the degrees of the heat of the iron...above the heat of the atmosphere, found by the thermometer, were in geometrical progression, when the times are in an arithmetical progression..."

Most heat transfer texts specify that the heat transfer coefficient calculated from Eq. (1) should be convective only, and it is clear from the statement "*the wind blew continually upon it*" that Newton had this mode of transfer in mind. However, since he stated that the piece of iron was "*red hot*", it is reasonable to assume that radiation played a significant role in the heat transfer process he was observing, and since it is a definition rather than a law there is no reason why Eq. (1) could not be used to define a coefficient that accounts for heat transferred by any mode. It is perhaps unsurprising then that the term "heat transfer coefficient" appears to have slightly different meanings, depending on its context, which often reflect the method by which the quantity was measured.

For modelling purposes, the heat transfer coefficient is often used simply as a boundary condition for conduction calculations, and hence there is no need to separate the total heat transferred into amounts transferred by each mode. Instead, "apparent" heat transfer coefficients, which include heat transfer by any mode, are often more practical to deal with than a strict convection heat transfer coefficient.

2.1. Back-calculation from transient temperature–time data

The most common method for determining heat transfer coefficients in convection ovens appears to be the "transient temperature measurement" method. This method involves fitting a mathematical model to transient temperature vs. time data and back-calculating the average the heat transfer coefficient. Eq. (2) is a general solution of the Heat Diffusion equation for an object with convective heat transfer at the surface:

$$Y = \sum_{j=1}^{\infty} f_j(Bi)\exp(-g_j(Bi)Fo) \tag{2}$$

where Y is a dimensionless temperature variable:

$$Y = \frac{T - T_\infty}{T_i - T_\infty} \tag{3}$$

Bi is the Biot number (the ratio of internal to external thermal resistance):

$$Bi = \frac{hX}{k} \tag{4}$$

Fo is the Fourier number (a dimensionless time variable):

$$Fo = \frac{kt}{\rho c X^2} \tag{5}$$

The functions $f_j(Bi)$ and $g_j(Bi)$ depend on the geometry of the object, and are specified in most heat transfer reference texts. For $Fo > 0.2$, only the first term in the series described by Eq. (1) is significant. Hence, using the appropriate geometry functions for a cube, Eq. (1) may be rewritten:

$$Y = \left(\frac{4\sin\beta}{2\beta + \sin 2\beta}\right)^3 \exp(-3\beta^2 Fo) \tag{6}$$

where β is the first root of:

$$\beta\tan\beta = Bi \tag{7}$$

If the logarithm of the fractional unaccomplished centre-temperature change is plotted against time, the linear portion of the plot may be fitted by Eq. (8):

$$\ln Y = B - st \tag{8}$$

By comparison of Eq. (8) with the Eq. (6):

$$3\beta^2 Fo = st \tag{9}$$

substituting for Fo, cancelling t, and rearranging for β:

$$\beta = \sqrt{\frac{s\rho c X^2}{3k_s}} \tag{10}$$

From Eqs. (4) and (7):

$$h = \frac{k_s\beta\tan\beta}{X} \tag{11}$$

Alternatively, if the Biot number of the object of interest is less than 0.1, then the lumped heat capacity approximation may be made (Holman, 1992), in which case Eq. (6) may be simplified to:

$$Y = \exp(-BiFo) \tag{12}$$

where the ratio V/A is used as the characteristic dimension when calculating Bi and Fo. The heat transfer coefficient may be calculated from Eq. (13):

$$h = \frac{s\rho_s V c_s}{A} \tag{13}$$

The heat transfer coefficients measured by this method will include both convective and radiative heat transfer, and so the data must be corrected if convective heat transfer coefficients are required. It is assumed that the measured (apparent) heat transfer coefficient (h_a) is the sum of the convective coefficient (h_c) and the radiative coefficient (h_r):

$$h_a = h_c + h_r \tag{14}$$

The radiative heat transfer coefficient may be estimated by Eq. (15):

$$h_r = F\varepsilon\sigma(T_s + T_\infty)(T_s^2 + T_\infty^2) \tag{15}$$

and hence the convective coefficient may be calculated by substituting Eq. (15) into (Eq. (14)):

$$h_c = h_a - F\varepsilon\sigma(T_s + T_\infty)(T_s^2 + T_\infty^2) \tag{16}$$

2.2. Mass-loss-rate and psychrometry methods

Kondjoyan and Daudin (1993) derived equations for calculating heat transfer coefficients during the steady state or 'constant rate' period of a drying process, using wetted plaster samples. The constant rate drying period is characterised by a constant rate of mass loss from the object and a steady surface temperature. During this period there is no net change in the surface temperature because the heat arriving at the surface evaporates moisture rather than adding sensible heat to the object:

$$q_{conv} + q_{rad} + q_{evap} = 0 \tag{17}$$

or:

$$h_c(T_\infty - T_s) + F\varepsilon\sigma(T_\infty^4 - T_\infty^4) + \Phi L(T_s) = 0 \tag{18}$$

where Φ is the mass loss per unit surface area ($kg\,s^{-1}\,m^{-2}$) and $L(T_s)$ is the enthalpy of vaporisation of water at the surface temperature. The apparent heat transfer coefficient during the steady state period may be calculated from Eq. (19):

$$h_a = \frac{-\Phi L(T_s)}{(T_\infty - T_s)} \tag{19}$$

The convection heat transfer coefficient may be calculated from Eq. (20):

$$h_c = \frac{-\Phi L(T_s)}{(T_\infty - T_s)} - \frac{F\varepsilon\sigma(T_\infty^4 - T_s^4)}{(T_\infty - T_s)} \quad (20)$$

Based on the mass-loss-rate method and the Chilton–Colburn analogy between convective heat and moisture transfer, Kondjoyan and Daudin also developed a method to measure local heat transfer coefficients by psychrometry, and without the inconvenience of measuring Φ. Assuming that the ratio of convective heat and mass transfer coefficients was constant, a parameter K was defined:

$$K = \frac{h_c}{\kappa L} = \frac{h_{c,local}}{\kappa_{local} L(T_s)} \quad (21)$$

where κ was a mass transfer coefficient defined by:

$$\kappa = \frac{\Phi}{p_{dew} - p_s} \quad (22)$$

Eq. (20) could therefore be rewritten to calculate the local convective heat transfer coefficient at the point where the surface temperature measurement is made:

$$h_{c,local} = \frac{F\varepsilon\sigma(T_\infty^4 - T_s^4)}{(T_s - T_\infty) + (p_s - p_{dew})/K} \quad (23)$$

The constant κ may be determined experimentally using Eqs. (20)–(22), or theoretically from a modification of the Chilton–Colburn analogy:

$$\frac{h_c}{\kappa} = c\frac{M_{air}P}{M_{water}}\left(\frac{Sc}{Pr}\right)^{2/3} \quad (24)$$

2.3. Heat flux sensors

Local heat transfer coefficients may be determined using heat flux sensors which measure the temperature difference across a thin thermal resistor. The heat transfer coefficient is then calculated from the heat flux divided by the temperature difference between the surface and the ambient air. *Micro-Foil*™ (RdF Corporation, 23 Elm Avenue, Hudson, New Hampshire 03021-0490) sensors were used in this study. The heat flux output signal, E (μV), was converted to W m^{-2} by a calibration factor (C) and then corrected for the appropriate surface temperature with a factor ($\theta(T_s)$). Hence, the heat transfer coefficient was calculated from Eq. (25):

$$h_a = \frac{EC\theta(T_s)}{(T_\infty - T_s)} \quad (25)$$

Each sensor was individually calibrated by the manufacturers prior to shipping. The heat flux sensor provided a continuous measure of the heat transfer at the sensor position; however, it was not suitable for use with the wet samples since it prevented moisture from evaporating.

2.4. Nusselt number correlations

Convective heat transfer coefficients may be estimated from empirical correlations based on the velocity and physical properties of air, the temperature and the geometry of the samples. Eq. (26) is the commonly accepted Nusselt correlation for predicting average heat transfer coefficient values for low velocities in flat plate geometries (Table 7.9, Incropera & De Witt, 2002).

$$Nu = 0.665Re^{1/2}Pr^{1/3} \quad (26)$$

3. Materials and method

A series of heat transfer coefficient measurements were performed involving two plaster cubes; one was dry with a thermocouple placed at the centre and a heat flux sensor on one of the faces, the other was completely saturated and had three thermocouples placed at different positions on one of the cube faces.

3.1. Plaster samples

Calcium sulphate is an abundant mineral which occurs naturally in different states of hydration (Kirk & Othmer, 1994). The most common form is the dihydrate ($CaSO_4 \cdot 2H_2O$) also known as gypsum. When gypsum is heated above approximately 128 °C it is converted to the hemihydrate form ($CaSO_4 \cdot 1/2H_2O$) sometimes referred to as "Plaster of Paris" or "bassanite". When heated above approximately 163 °C the remaining water of crystallisation is removed and the anhydrous form is known as "Anhydrite". Plaster was chosen as the experimental material because it allowed for the effects of evaporative heat transfer to be examined, since, when saturated, plaster retains a surface water activity of 1.0 for a long time (Kondjoyan & Daudin, 1993). Another advantage of using plaster was that the samples could be moulded into regular shapes (cubes), which were convenient for performing heat transfer calculations.

The plaster samples were prepared by mixing 85 parts water with 100 parts gypsum powder by mass. Half of the samples were dried at temperatures below 100 °C until their masses stopped decreasing, while the other samples were placed in plastic bags to prevent them losing moisture. Specific heat capacity, thermal conductivity and emissivity data for gypsum/Plaster of Paris were either measured or obtained from the literature and are shown in Table 1.

3.2. Apparatus

Two ovens were used in the experiments; the first was a modified domestic fan oven fitted with load cells to measure the weight change of the samples as they dried

Table 1
Physical properties of plaster

		Dry plaster		Wet plaster		Source
ρ	(kg m^{-3})	790	±1%	1485	±1%	Measured
ε		0.91		0.91		(Incropera and De Witt, 2002)
α	(m s^{-2})	1.52×10^{-7}	±5%	2.56×10^{-7}	±10%	Measured
c	(J kg^{-1} K^{-1})	1140	±2%	2430	±2%	(Perry and Green, 1997)
k	(W m^{-1} K^{-1})	0.14	±5%	0.92	±10%	(Calculated from ρ,α, c)

(Fig. 1), the second was a *Maurer*™ *Rondette* commercially sized oven (Fig. 2). Temperatures were measured with *T*-type thermocouples, and the humidity within the oven was measured with an *Elektronik*™ *EE31* dew-point sensor. Air velocities within the ovens were measured with a *Dantec Flowmaster*™ hot-wire anemometer. Other than the air velocity measurements, all measurements were recorded by a *Hewlett Packard*™ data logger.

Fig. 1. Domestic fan oven used in experiments.

Fig. 2. Commercial oven used in experiments.

In the domestic oven, the samples were held in cages suspended from the load cells (Fig. 3). The dry sample had a heat flux sensor attached to the middle of one face, and a thermocouple placed at its centre. The heat flux sensor was attached to the plaster with heat transfer

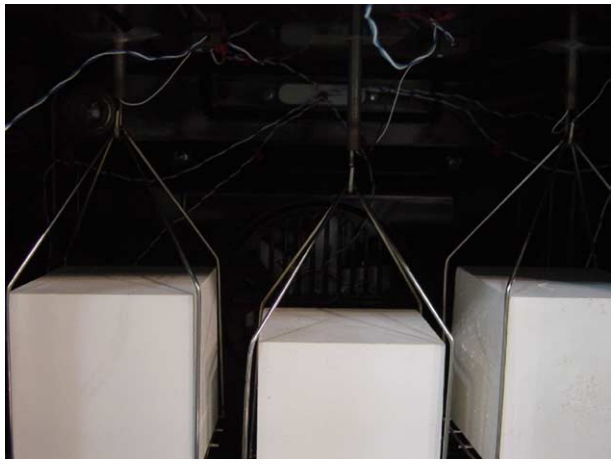

Fig. 3. Sample holders attached to load cells.

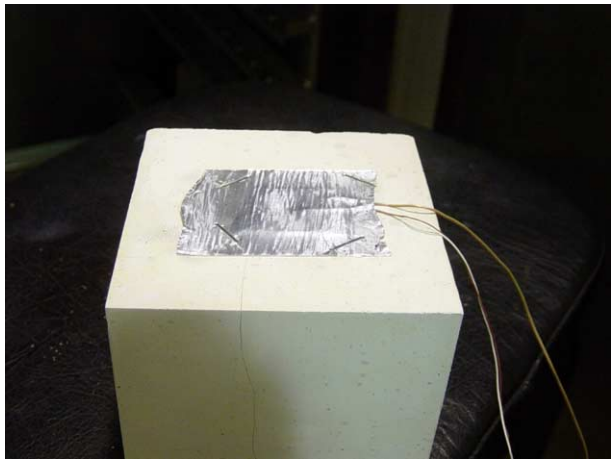

Fig. 4. Heat flux sensor attached to dry plaster sample.

paste and covered with a layer of aluminium tape (Fig. 4). The saturated cubes had three thermocouples placed at different positions just under the surface. The setup was the same for the commercial oven apart from the load cells which could not practically be fitted into the oven.

4. Results and discussion

4.1. Domestic fan oven

Velocities within the domestic fan oven varied between 0.1 and 0.7 m s^{-1}, and temperatures within the oven varied between 20 and 170 °C. Under these conditions convective heat transfer coefficients between 4 and 10 W m^{-2} K^{-1} were predicted by Eq. (26). Eq. (26) assumes laminar flow; however, due to the geometry of the oven and the mixing action of the fan, unsteady, turbulent flows would exist even for relatively low velocities. Eq. (27) is recommended for flat plate geometries under mixed flow conditions (Incropera & De Witt, 2002); however, the Nusselt Numbers predicted by this correlation were negative for the range of velocities encountered in the oven.

$$Nu = (0.037Re^{4/5} - 871)Pr^{1/3} \quad (27)$$

The presence of turbulence would most likely increase heat transfer rates, and therefore Eq. (26) would probably underestimate the value of heat transfer coefficients.

Figs. 5 and 6 show temperature data recorded during typical experimental runs for two different oven temperatures (T_∞). An obvious feature of these results is the very loose temperature control of the oven, evidenced by typical fluctuations of 20 °C, but sometimes as much as 30 °C (Fig. 5). Fig. 6 shows that the centre temperature of the dry cube rose above the oven temperature, which was not an uncommon observation for higher oven temperatures and suggested that heat was being generated within the plaster. This was most likely caused by moisture absorption by the dry cube and the subsequent exothermic change in crystallisation state from hemihydrate to dihydrate. This feature coupled with the high fluctuation in the oven temperature meant that the Eq. (6) was not a valid model for most of the runs, and rather than attempt to derive a model that incorporated the heat generation and oven temperature fluctuations, the transient temperature method was not used other than for selected runs at low temperatures. Of the runs that were successful, the apparent heat transfer coefficients ranged between 10 and 16 W m^{-2} K^{-1}.

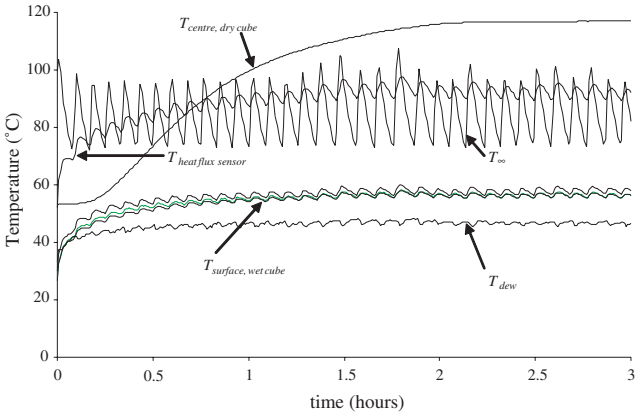

Fig. 6. Temperature data recorded during typical experimental run ($\overline{T}_\infty = 46\,°C$).

Fig. 7 shows plots of the apparent heat transfer coefficients (h_a) calculated from the heat flux sensor output data using to Eq. (25), and the temperature difference between the oven and the heat flux sensor ($T_\infty - T_s$). The high fluctuation in the oven temperature meant that the ($T_\infty - T_s$) term periodically approached zero and after approximately the first 30 min, alternated between having positive and negative values (Figs. 5 and 6). Therefore even a slight lag between the times at which E and T_s were recorded caused the calculated value of h_a to approach ∞ whenever ($T_\infty - T_s$) approached zero,

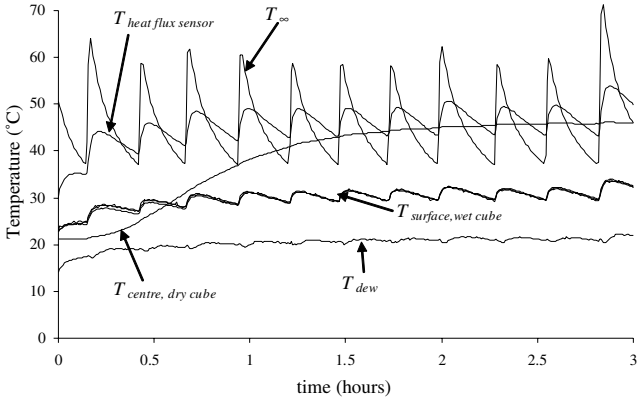

Fig. 5. Thermocouples placed at surface of wet plaster.

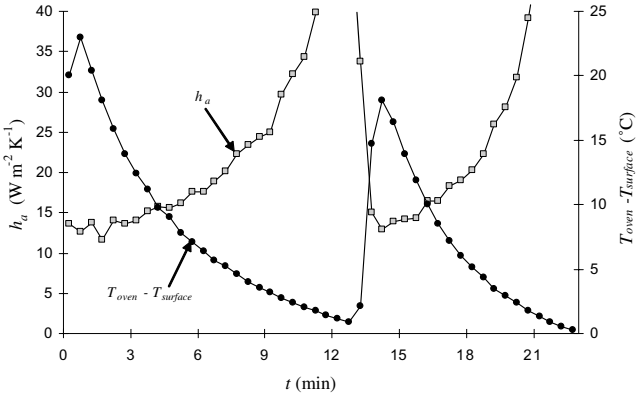

Fig. 7. Temperature data recorded during typical experimental run ($\overline{T}_\infty = 85\,°C$).

as shown in Fig. 7. However, the majority of the h_a values calculated from the heat flux sensor were between 10 W m^{-2} K^{-1} and 30 W m^{-2} K^{-1}.

The heat transfer coefficients calculated from the mass-loss-rate method according to Eq. (19) were least affected by the loose temperature control of the oven. Although the surface temperatures of the wet cubes clearly fluctuated in response to the oven temperature (Figs. 5 and 6), the average value of $(T_\infty - T_s)$ during the *constant rate* period was used in the calculations, and therefore the effects of the fluctuations were cancelled out over time. The temperature fluctuations did not significantly affect the rate of moisture loss either, which was indeed constant during the *constant rate* period (Fig. 8). The major uncertainty involved in the use of Eq. (19) was that T_s was based on the average of the temperatures measured at three thermocouple positions, rather than the temperature distribution integrated over the entire surface of the cube (refer to Eq. (24) of Kondjoyan & Daudin, 1993). A measure of this uncertainty

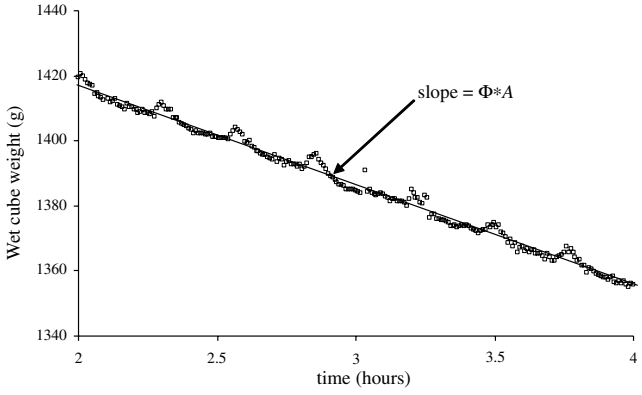

Fig. 8. Apparent heat transfer coefficients (h_a) calculated from the heat flux sensor output data.

was obtained by comparing the difference between h_a calculated from T_s at a single point, and the average T_s from the three sensor positions. This value ranged between 5% at the lowest oven temperature and 2% at the highest oven temperature.

Table 2 shows the average apparent heat transfer coefficients measured by the mass-loss-rate method for a range of oven temperatures, as well as the convective and radiative heat transfer coefficients calculated using Eqs. (19) and (20), and the measured values of the parameter K. The view factor F was assumed to be 1.0 in all the radiation calculations, and the emissivity of the plaster was assumed to be independent of temperature.

Table 2 shows a gradual increase in h_a with oven temperature which was attributed to the increase in the significance of radiation. The convective heat transfer coefficient h_c appeared to decrease slightly with temperature, which was contrary to what was expected; however, this may be due to overestimation of h_r by Eq. (15), since the maximum value for the view factor was assumed. The h_a data obtained by the mass-loss-rate method were of similar magnitude to the data obtained by the heat flux sensor.

Fig. 9 shows a comparison of the measured values of K with theoretical values predicted using Eqs. (21) and (24) as a function of T_∞. The measured K-values are higher than the predicted values, and also had a stronger dependence on temperature. The exponent in Eq. (24) is essentially an empirical factor, and although a value of 2/3 has been measured by many experimenters (Table 1, Kondjoyan & Daudin, 1993), it may not be the appropriate value for this situation. The majority of the experimental work examining the Chilton–Colburn analogy occurred in steady flow conditions at temperatures typically below 50 °C, and so high uncertainties would be

Table 2
Heat transfer coefficient data measured by mass-loss-rate method for domestic oven

T_∞ (°C)	$\overline{T}_s$ (°C)	T_d (°C)	h_a (W m^{-2} K^{-1})	h_c (W m^{-2} K^{-1})	h_r (W m^{-2} K^{-1})	K (Pa K^{-1})
43.6	28.6	16.8	24	18	6	101.1
44.5	28.9	17.1	24	18	6	97.1
45.7	31.2	21	24	18	6	104.9
45.6	30.9	19.9	24	18	6	108
48.0	30.6	18.6	24	18	6	96.5
85	56.9	46.9	24.5	16	8.5	154.3
84.1	54.9	43.3	25	16.5	8.5	156.7
86.5	48.3	24.2	25.5	17.5	8	148.6
84.4	55.3	43.7	22.5	14	8.5	152
85	55.5	43.7	22.5	14	8.5	153.2
85.8	55	43.6	23	15	8	144.5
102.9	58.9	43.4	25	16	9	145.4
127	69.3	53.3	26	15	11	158.9
135.7	79.3	67.2	27.5	16	11.5	191.7
133.5	80	67.5	28	16.5	11.5	215.2
132.4	76.3	64	28	17	11	181.7
134	82.4	71.5	27	15	12	213.1

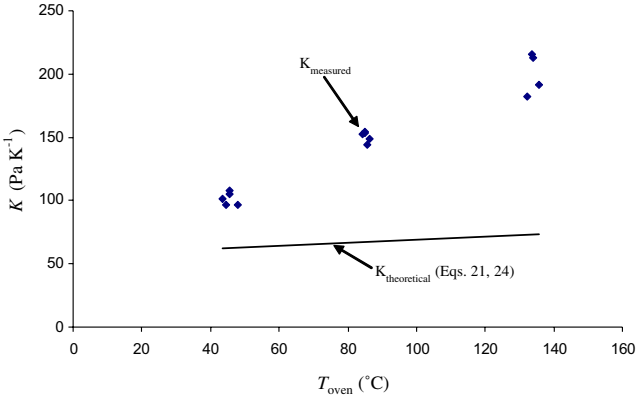

Fig. 9. Comparison of the measured values of K with theoretical values.

expected when applying Eq. (24) to higher temperatures and random flow patterns.

4.2. Commercial oven

Velocities within the domestic oven varied between 0.2 and 1.9 m s^{-1}, and therefore, according to Eq. (26), convective heat transfer coefficients between 6 and 17 W m^{-2} K^{-1} would be expected, for temperatures between 0 and 180 °C. The apparent heat transfer coefficient measured by the heat flux sensor were in similar range to those measured in the domestic oven; between 10 W m^{-2} K^{-1} and 40 W m^{-2} K^{-1}.

Since the mass loss rates from the wet cubes could not be measured in the commercial oven, the psychrometry method was applied, using the experimental values of K measured in the domestic oven. However, the heat transfer coefficients calculated from Eq. (23) were much higher than those measured by the heat flux sensor and had negative values when the oven temperature was above 100 °C. This was attributed to error in the K values, since small changes in K had a significant effect on h_c calculated from Eq. (23), as shown in Fig. 10 which is a plot of the dependence of h_c on K for an oven temperature of 142.6 °C, a surface temperature of 94.7 °C, and a dew point temperature of 92.1 °C. Since humidity control was not possible within the domestic oven, no measure of the dependence of K on humidity was obtained.

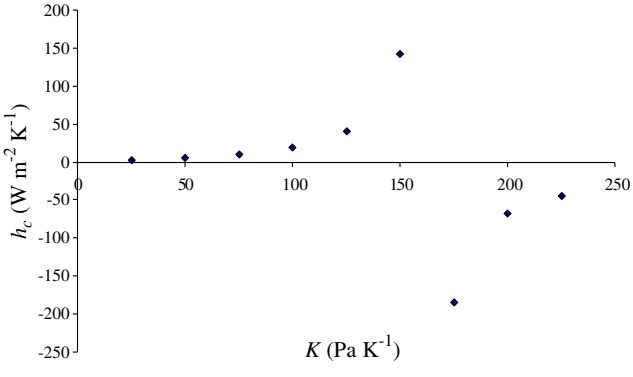

Fig. 10. Plot of the dependence of h_c on K.

4.3. Efficacies of the different measurement methods

The most reliable heat transfer coefficient data was obtained from the heat flux sensor and the mass-loss-rate method. Direct numerical comparisons between the data from the two methods was not warranted since the emissivity of the aluminium tape placed over the heat flux sensor (Fig. 4) would be much lower than that of plaster, and because the heat flux sensor was not measuring the effect of evaporation. However, the data were in relative agreement as may be seen from a comparison between the data in Fig. 7 and Table 2.

Although commonly used, the transient temperature method was the least useful method in these experiments, because it was affected significantly by the temperature fluctuations of the oven air. Plaster was clearly not a suitable material for this method, since it could absorb moisture and because the Biot number of the samples (between 5 and 10) was much higher than preferable. The rationale for using plaster was to provide a means for a direct comparison between the data obtained from samples with and without evaporative heat transfer, but unfortunately this was not achieved. However, even with a more suitable material, such as copper or aluminium, the effects of the fluctuating temperature would have made use of Eq. (6) difficult, and since several measurements would be required, the process would be cumbersome.

By contrast, the heat flux sensor provided similar data to that which could be expected from a successfully implemented transient temperature method, but with much less effort. Another advantage of the heat flux sensor was that it could measure the time variation of the heat transfer coefficient, unlike the other methods.

The mass-loss-rate method required a measurement of the mass lost by the samples, which meant it was not the most practicable method, but it had the major advantages of being a very direct measurement, and being able to measure the effects of evaporation. The heat transfer processes occurring in the wet plaster cubes provided a much closer analogy to cooking meat than the dry cubes, and hence data obtained from this method would be more similar to heat transfer coefficients encountered in meat cooking processes.

In principle, the psychrometry method should provide the benefits of the mass-transfer-rate method without the difficulty of having to measure the mass of the samples; however, the experiments performed in this study suggested that neither the K values obtained from theoretical relationships, nor those measured experimentally in a different environment could be relied upon to give accurate results for a given oven.

4.4. Implications for cooking models

An approach that is sometimes used when testing heat transfer models is to adjust the heat transfer coefficient until the model fits the experimental data; however, this is a somewhat dubious approach since it may disguise errors in the model, and certainly does not validate it. In a genuine validation process the heat transfer coefficient should be measured independently.

Depending on the dimensions of the meat product being cooked, the Biot number will be in a range such that the uncertainty in the heat transfer coefficient will significantly affect the accuracy of the model. Under these circumstances a direct measurement of the heat transfer coefficient would most likely be beneficial. Based on the results of this study, the best method to use would be the mass-loss-rate method.

5. Conclusions

Of the methods used in this study to measure apparent heat transfer coefficients, the heat flux sensor method was the easiest to implement, while the data produced by the mass-loss-rate method were the most reliable and would be most applicable to the oven cooking of meat. The apparent heat transfer coefficients measured in the domestic oven by the mass-loss-rate method ranged between 22 and 28 $W m^{-2} K^{-1}$, depending on the oven temperature. The mass-loss-rate method could not be implemented in the commercial oven, and the psychrometric method, which is based on the mass-loss-rate method, was not applied successfully either. The majority of the measurements made by the heat flux sensor in the commercial oven varied between 15 and 40 $W m^{-2} K^{-1}$.

Acknowledgment

This work was funded by the *Foundation for Research, Science and Technology* (New Zealand) as part of Objective 2 of Contract C10X0201.

References

Anon. (2001). *Market report: ready meals*. Published by Key Note Ltd (http://www.mindbranch.com/page/catalog/product/2e6a73703f636f64653d523331302d303234342670617274 6e65723d30.html).

Burfoot, D., & Self, K. P. (1988). Prediction of heating times for cubes of beef during water cooking. *International Journal of Food Science and Technology, 23*, 247–257.

Chang, H. C., Carpenter, J. A., & Toledo, R. T. (1998). Modeling heat transfer during oven roasting of unstuffed turkeys. *Journal of Food Science, 63*(2), 257–261.

Chen, H., Marks, B. P., & Murphy, R. Y. (1999). Modeling coupled heat and mass transfer for convection cooking of chicken patties. *Journal of Food Engineering, 42*(3), 139–146.

Dagerskog, M. (1979). Pan-frying of meat patties I: A study of heat and mass transfer. *Lebensmittel-Wissenschaft und Technologie, 12*(4), 217–224.

Fellows, P. J. (2000). *Food processing technology principles and practice* (2nd ed.). Cambridge: Woodhead Publishing Limited.

Holman, J. P. (1992). Heat transfer in SI Units (7th ed.). London: McGraw-Hill Book Company.

Houšová, J., & Topinka, P. (1985). Heat transfer during contact cooking of minced meat patties. *Journal of Food Engineering, 4*, 169–188.

Ikediala, J. N., Correia, L. R., Fenton, G. A., & Ben-Abdallah, N. (1996). Finite element modelling of heat transfer in meat patties during single-sided pan-frying. *Journal of Food Science, 61*(4), 796–802.

Incropera, F. P., & De Witt, D. P. (2002). *Fundamentals of heat and mass transfer*. New York: Wiley.

Jakob, M. (1947). *Heat transfer*. New York: Wiley.

Kirk, R. E., & Othmer, D. F. (1994). *Encyclopedia of chemical technology* (Vol. 12). New York: John Wiley & Sons.

Kondjoyan, A., & Daudin, J. D. (1993). Determination of transfer coefficients by psychrometry. *International Journal of Heat and Mass Transfer, 36*(7), 1807–1818.

Neff, J. (1997). HMR: Getting it there from here. *Food Processing, 58*(6), 27–36.

Newton, I. (1701). Scala graduum caloris. *Philosophical Transactions of the Royal Society (London), 22*, 824–829, Translated from Latin to English in: Cohen, I. B. (1978). *Isaac Newton's Papers & Letters on Natural Philosophy* (2nd ed.). Cambridge, Massachusetts: Harvard University Press, pp. 265–268.

Obuz, E., Powell, T. H., & Dikeman, M. E. (2002). Simulation of cooking cylindrical beef roasts. *Lebensmittel-Wissenschaft und Technologie, 35*(8), 637–644.

Pan, Z., & Singh, R. P. (2002). Heating surface temperature and contact-heat transfer coefficient of a clam-shell grill. *Lebensmittel-Wissenschaft und-Technologie, 35*(4), 348–354.

Pan, Z., Singh, R. P., & Rumsey, T. R. (2000). Predictive modelling of contact-heating process for cooking a hamburger patty. *Journal of Food Engineering, 46*, 9–19.

Perry, R. H., & Green, D. W. (1997). *Perry's chemical engineers' handbook* (7th ed.). New York: McGraw-Hill.

Singh, N., Akins, R. G., & Erickson, L. E. (1984). Modeling heat and mass transfer during the oven roasting of meat. *Journal of Food Process Engineering, 7*, 205–220.

Verboven, P., Datta, A. K., Anh, N. T., Scheerlink, N., & Nicolaï, B. M. (2003). *Journal of Food Engineering, 59*(2–3), 181–190.

Whichchukit, S., Zorilla, S., & Singh, R. P. (2001). Contact heat transfer coefficient during double-sided cooking of hamburger patties. *Journal of Food Processing Preservation, 25*, 207–221.